

# Magnetic and magnetoelastic properties of $\text{UCo}_2\text{Si}_2$ as studied by high-field magnetization and ultrasound measurements

A. V. Andreev,<sup>1,\*</sup> S. Yasin,<sup>2</sup> Y. Skourski,<sup>2</sup> A. A. Zvyagin,<sup>3,4</sup> S. Zherlitsyn,<sup>2</sup> and J. Wosnitzer<sup>2</sup>

<sup>1</sup>*Institute of Physics ASCR, Na Slovance 2, 18221 Prague 8, Czech Republic*

<sup>2</sup>*Dresden High Magnetic Field Laboratory, Helmholtz-Zentrum Dresden-Rossendorf and TU Dresden, D-01314 Dresden, Germany*

<sup>3</sup>*Max-Planck-Institut für Physik komplexer Systeme, Nöthnitzer Strasse, 38, D-01187 Dresden, Germany*

<sup>4</sup>*B. I. Verkin Institute for Low Temperature Physics and Engineering of the National Academy of Sciences of Ukraine, Lenin Avenue 47, Kharkov 61103, Ukraine*

(Received 1 March 2013; published 10 June 2013)

We investigated an antiferromagnet  $\text{UCo}_2\text{Si}_2$  by use of magnetization and ultrasound measurements in pulsed magnetic fields up to 60 T. It is found that the crystal  $\text{UCo}_2\text{Si}_2$ , which has the antiferromagnet type-I magnetic structure in zero field below  $T_N = 83$  K, undergoes the metamagnetic phase transition to ferrimagnetic structure  $++-$  type similarly to the  $\text{UNi}_2\text{Si}_2$  with substitution of 10%–15% Ni by Pd or  $\text{UPd}_2\text{Si}_2$ . Therefore, similar phase transitions take place in the compounds with expected essentially different strength of the  $5f$ - $d$  electron hybridization. In  $\text{UCo}_2\text{Si}_2$ , the transition occurs when the magnetic field is applied along the  $c$  axis at 45 T (at 1.5 K). The transition is extremely sharp and exhibits a small but non-negligible hysteresis. With increasing temperature, it becomes broader and vanishes at  $T_N$ . In our ultrasound measurements, the metamagnetic transition appears as anomalies in the sound velocity and attenuation. Our analysis suggests that the low-temperature changes in the sound velocity and attenuation predominantly are determined by an exchange renormalization caused by the sound waves.

DOI: [10.1103/PhysRevB.87.214409](https://doi.org/10.1103/PhysRevB.87.214409)

PACS number(s): 75.30.-m, 75.50.Ee, 62.65.+k

## I. INTRODUCTION

Uranium ternary intermetallics of the composition  $\text{UT}_2\text{X}_2$ , where  $T$  is a late  $3d$ ,  $4d$ , or  $5d$  metal and  $X$  is a  $p$ -electron element (Si or Ge), crystallizing in two related structure types, form one of the widest group of actinide compounds whose magnetic and other electronic properties were studied systematically. These materials exhibit a large variety of magnetic states starting from antiferromagnetic ( $\text{UCr}_2\text{Si}_2$ ), complex ferrimagnetic ( $\text{UNi}_2\text{Si}_2$ ), and ferromagnetic structures ( $\text{UCu}_2\text{Si}_2$ ), through Pauli paramagnets ( $\text{UFe}_2\text{Si}_2$ ), and, finally, to one of the most intriguing cases,  $\text{URu}_2\text{Si}_2$ , where heavy-fermion superconductivity combines with so-called hidden order.<sup>1–3</sup> One representative of this group is  $\text{UCo}_2\text{Si}_2$ , that crystallizes in the body-centered version of the  $\text{UT}_2\text{X}_2$  structures, i.e., the tetragonal  $\text{ThCr}_2\text{Si}_2$ -type structure (space group  $I4/mmm$ ). The structure is formed by U, Co, and Si basal-plane atomic layers stacked along the  $c$  axis.  $\text{UCo}_2\text{Si}_2$  is antiferromagnetic (AF) below the Néel temperature  $T_N = 83$  K. The magnetic structure obtained by use of powder neutron diffraction experiments consists of ferromagnetic basal-plane layers of U magnetic moments  $M_U$  with  $1.42 \mu_B$  (at 4.2 K) oriented parallel to the  $c$  axis, that are coupled in an alternating  $+-+-$  sequence (AF type-I structure) along that axis.<sup>4</sup> The Co atoms carry no magnetic moment. This simple magnetic structure persists down to the lowest temperatures without any order-order transition that often occurs in uranium-containing magnets. The magnetic moments are carried only by the U atoms.

Magnetization (up to 14 T), electrical resistivity, and specific heat performed on single-crystalline sample  $\text{UCo}_2\text{Si}_2$  have been studied in Refs. 5,6. At low temperatures, the magnetic susceptibility in  $\text{UCo}_2\text{Si}_2$  measured along the main axes is almost identical, i.e., the compound is magnetically

nearly isotropic. However, with increasing temperature the uniaxial magnetic anisotropy grows and is preserved even in the paramagnetic state.<sup>6</sup> As in many other U intermetallics, in particular in the  $\text{UT}_2\text{X}_2$  group, the magnetic susceptibility of  $\text{UCo}_2\text{Si}_2$  above the ordering temperature is much larger along the moment direction (the  $c$  axis in  $\text{UT}_2\text{X}_2$ ) than along the basal plane and obeys a Curie-Weiss law (with effective moment  $\mu_{\text{eff}} = 2.55 \mu_B$  and paramagnetic Curie temperature  $\Theta_p = -29$  K). The magnetic susceptibility along the  $a$  axis is smooth, does not obey a Curie-Weiss law, and shows only a small anomaly at  $T_N$ .<sup>6</sup>  $T_N$  is reduced by  $\sim 2$  K in a magnetic field of 14 T applied along the  $c$  axis, while there is no such effect for a magnetic field applied in the basal plane. Under pressure,  $T_N$  has been found to decrease and the estimated relatively low critical pressure ( $\sim 8$  GPa) for the loss of magnetic order in  $\text{UCo}_2\text{Si}_2$  points to an itinerant character of the magnetism.<sup>5,6</sup>

Other  $\text{UT}_2\text{X}_2$  compounds exhibit more evolved magnetic phase diagrams than  $\text{UCo}_2\text{Si}_2$ . In particular,  $\text{UNi}_2\text{Si}_2$  has three ordered phases: a ferrimagnetic, an AF type-I, and an incommensurate AF phase. In the ferrimagnetic ground state, the magnetic moments show a  $++-$  sequence with longitudinally modulated magnitude resulting in a spontaneous moment of  $0.53 \mu_B$ ,  $1/3$  of  $\mu_U$ .<sup>7,8</sup> Substitution of 10%–15% Ni by Pd stabilizes the AF type-I structure, and the ferrimagnetic  $++-$  arrangement is restored after a metamagnetic transition above about 5 T. This state persists even after the field is released to zero.<sup>9</sup> The  $++-$  phase is also observed at high magnetic fields in  $\text{UPd}_2\text{Si}_2$  (having an AF type-I structure at zero field, such as  $\text{UCo}_2\text{Si}_2$ ). The transition occurs at a critical field of 15 T and is accompanied by a huge hysteresis and relaxation effects.<sup>10,11</sup>

The most important mechanism determining magnetic and other electronic properties of actinide (in particular, uranium)

compounds is hybridization of  $5f$  electrons with electrons of ligands (under the condition that actinide atoms are separated far enough from each other to prevent direct overlap of  $5f$  electron shells).<sup>1</sup> It is especially effective in the case of ligands with  $3d$ ,  $4d$ , and  $5d$  electrons. It is generally accepted that the hybridization decreases in the sequence  $T = \text{Fe, Co, Ni}$  in the isostructural series of the  $U$ - $T$ - $X$  compounds. A similar trend is also observed in compounds with  $4d$  and  $5d$  metals in sequences  $T = \text{Ru, Rh, Pd}$  and  $\text{Os, Ir, Pt}$ . This leads to a suppression of  $M_U$  down to zero for  $T = \text{Fe, Ru, and Os}$  (strong hybridization), a magnetically ordered state with moderate  $M_U$  for  $T = \text{Co, Rh, and Ir}$ , and the formation of a relatively high  $M_U$  (however, still considerably lower than for single  $U^{3+}$  or  $U^{4+}$  ions) for  $T = \text{Ni, Pd, and Pt}$  (low hybridization). On the other hand, because just this hybridization is a very effective exchange mechanism, the ordering temperature for  $T = \text{Co}$  is higher than for  $T = \text{Ni}$ —for example,  $\text{UCoGa}$  with  $M_U = 0.7 \mu_B$ ,  $T_C = 48 \text{ K}$  vs  $\text{UNiGa}$  with  $M_U = 1.4 \mu_B$ ,  $T_N = 39 \text{ K}$ , or, in compounds of the  $UT_2X_2$  group,  $\text{UCo}_2\text{Ge}_2$  with  $M_U = 1.5 \mu_B$ ,  $T_C = 174 \text{ K}$  and  $\text{UNi}_2\text{Ge}_2$  with  $M_U = 2.35 \mu_B$ ,  $T_N = 77 \text{ K}$ .

However, influence of the  $5f$ - $d$  hybridization is not clear enough to explain all particular cases. In the compound under consideration,  $\text{UCo}_2\text{Si}_2$ , and its isostructural analog with lower hybridization,  $\text{UNi}_2\text{Si}_2$ ,  $M_U$  is approximately the same ( $1.4$ – $1.6 \mu_B$ ) whereas the ordering temperatures are  $83 \text{ K}$  (Co) and  $124 \text{ K}$  (Ni). Therefore, in contradiction with the general trend,  $T_N$  in  $\text{UNi}_2\text{Si}_2$  is considerably higher than in  $\text{UCo}_2\text{Si}_2$ . In  $\text{UPd}_2\text{Si}_2$ , where hybridization should be weaker,  $M_U$  is indeed higher,  $2.3 \mu_B$ , but the ordering temperature is even higher ( $136 \text{ K}$ ). All these three compounds exhibit (at some temperature interval) the same AF type-I magnetic structure. Since two of them have also the  $++-$  structure, either spontaneous ( $\text{UNi}_2\text{Si}_2$ ) or field-induced ( $\text{UPd}_2\text{Si}_2$ ), it is interesting whether  $\text{UCo}_2\text{Si}_2$  exhibits this ferrimagnetic phase in high magnetic fields as well.

Since uranium compounds, independent of their ground state, have typically very large magnetic anisotropies, their quantitative study requires high-quality single crystals (for which growth and characterization techniques are performed in the Prague laboratory) and the application of very high magnetic fields (available at the Dresden laboratory). Here, we present detailed results of high-field magnetization and magnetoacoustics studies performed on a  $\text{UCo}_2\text{Si}_2$  single crystal. Some preliminary data, together with experimental results for several other uranium antiferromagnetics, were briefly reported previously.<sup>12</sup>

## II. EXPERIMENT

The  $\text{UCo}_2\text{Si}_2$  single crystal was grown from a stoichiometric mixture of the pure elements (99.8% U, 99.9% Co, and 99.999% Si) by use of the Czochralski method using a triarc furnace with a water-cooled copper crucible and a tungsten rod as a seed. The pulling speed was  $10 \text{ mm/h}$ . The backscattered Laue patterns were used to check the monocrystalline state of the resulting ingot and to orient the crystal for cutting the samples for the magnetization and ultrasound measurements. The phase purity was checked by standard x-ray powder diffraction analysis on a part of the single crystal milled

into fine powder. It confirmed the tetragonal body-centered  $\text{ThCr}_2\text{Si}_2$ -type crystal structure with lattice parameters  $a = 392.1 \text{ pm}$  and  $c = 963.9 \text{ pm}$ , which are in agreement with literature data ( $a = 391.7 \text{ pm}$ ,  $c = 961.4 \text{ pm}$ ,<sup>4</sup>  $a = 390.8 \text{ pm}$ ,  $c = 963.7 \text{ pm}$ ).<sup>13</sup>

The magnetization measurements have been performed in pulsed magnetic fields up to  $60 \text{ T}$  applied along the  $a$  and  $c$  axes of a cubic crystal with side length of  $1.5 \text{ mm}$ . The rise time of the magnet pulse was  $7 \text{ ms}$  and the total pulse duration  $25 \text{ ms}$ . The magnet is energized by a  $1.44 \text{ MJ}$  capacitor module. The measurements were carried out at  $T = 1.5 \text{ K}$  and elevated temperatures. The magnetization was detected by an induction method with a standard pickup coil system. A more detailed description of the experimental setup is given in Ref. 14. The absolute values of the magnetization were calibrated from steady-field measurements up to  $14 \text{ T}$  in a PPMS-14 magnetometer (Quantum Design).

For the ultrasound measurements, two pairs of parallel facets were polished perpendicular to the  $a$  and  $c$  axes. A pair of piezoelectric film transducers was glued to the surfaces in order to excite and detect the acoustic waves in a frequency range of  $103$ – $107 \text{ MHz}$ . The measurements were performed using a pulse-echo technique.<sup>15</sup> A longitudinal geometry was used for the measurements, i.e., the polarization vector  $\mathbf{u}$  of the sound wave was parallel to the propagation vector  $\mathbf{k}$ , both being along the  $a$  axis. Magnetic fields up to  $64 \text{ T}$  were applied along the  $c$  axis. The relative changes of the sound velocity and sound attenuation have been measured in a  $^4\text{He}$  flow cryostat. The absolute value of the sound velocity at  $1.5 \text{ K}$  in zero magnetic field is  $5159 \text{ m/s}$ . All relative sound-velocity changes,  $\Delta v/v$ , presented below refer to this value.

## III. RESULTS AND DISCUSSION

Figure 1 shows the temperature dependence of the sound velocity and attenuation in zero magnetic field. Well-pronounced anomalies occur at the AF ordering. The sound-velocity change  $\Delta v/v$  shows a dip of  $1.2\%$  reflecting a pronounced softening of the lattice, whereas the sound attenuation change,  $\Delta\alpha$ , exhibits a sharp peak of  $6 \text{ dB/cm}$  reflecting a pronounced energy dissipation at the transition. Both effects prove a strong magnetoelastic coupling in  $\text{UCo}_2\text{Si}_2$ . The maximum in  $\Delta\alpha$  and the minimum in  $\Delta v/v$  appear at  $83 \text{ K}$ , in agreement with anomalies in other properties observed earlier,<sup>5,6</sup> e.g., specific heat  $C_p$  (bottom of Fig. 1). When comparing our results with those for  $\text{UCuGe}$ , another uranium-containing antiferromagnet, we also find a  $\lambda$ -type minimum at  $T_N$  in the longitudinal sound velocity of exactly the same value ( $1.2\%$ ) as in  $\text{UCo}_2\text{Si}_2$  and a somewhat larger maximum of  $25 \text{ dB/cm}$  in  $\Delta\alpha$ .<sup>16</sup> In the isostructural compound  $\text{UNi}_2\text{Si}_2$ , the observed minimum in  $\Delta v/v$  is more than one order of magnitude smaller with, in addition, a somewhat different temperature dependence. This is, however, for the sound geometry  $\mathbf{k}||\mathbf{u}||c$ .<sup>17</sup> Since, in addition, the ordered state below  $T_N$  in  $\text{UNi}_2\text{Si}_2$  is not the AF type-I structure but incommensurate, this difference is not surprising.

Magnetization data measured along the principal axes at  $1.5 \text{ K}$  are shown in Fig. 2. In field applied along the  $c$  axis, a magnetization jump is observed at the critical field  $\mu_0 H_{\text{cr}} = 45 \text{ T}$ . This metamagneticlike transition is

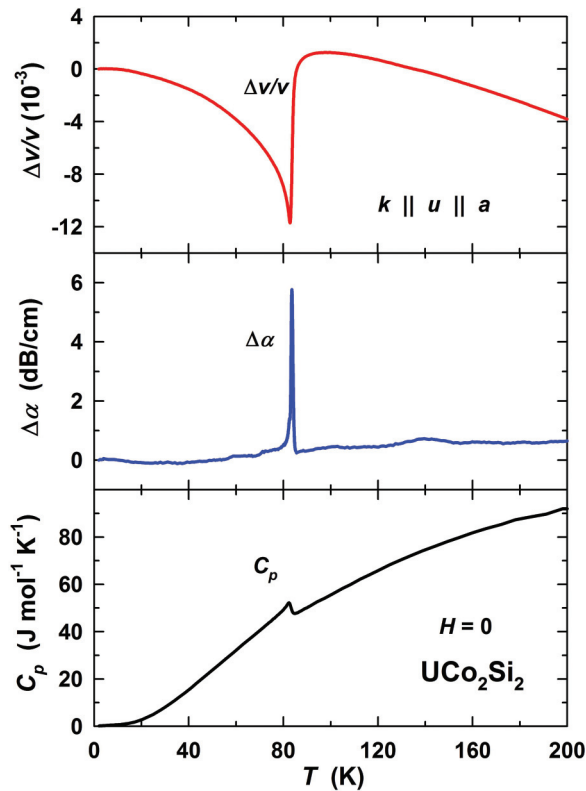


FIG. 1. (Color online) Temperature dependence of the relative changes of the sound velocity,  $\Delta v/v$ , and of the sound attenuation,  $\Delta\alpha$ , compared with specific heat,  $C_p$  (taken from Ref. 6).

very sharp. As seen in the inset of Fig. 2, the transition shows a hysteresis. Remarkably, this hysteresis is rather small ( $\mu_0\Delta H_{\text{cr}} = 0.16$  T), especially if we compare it with the huge hysteresis of an analogous transition in  $\text{UPd}_2\text{Si}_2$ , where  $\mu_0\Delta H_{\text{cr}}$  is larger than 15 T, so that  $\Delta H_{\text{cr}}$  is practically equal to  $H_{\text{cr}}$ .<sup>10,11</sup> Generally speaking, the sharpness of the transition,

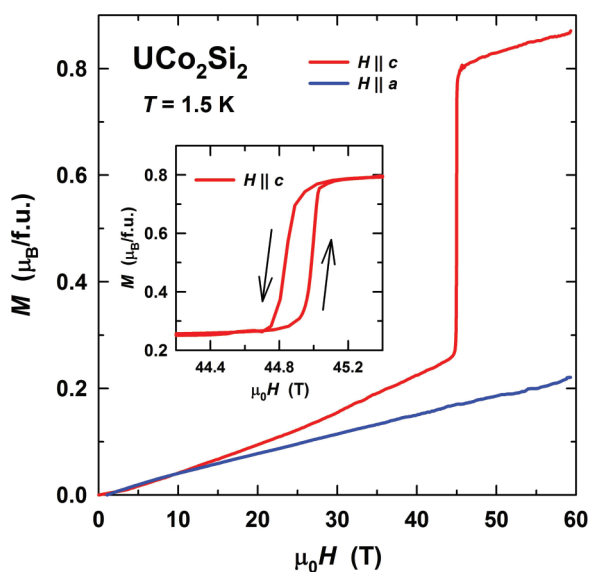


FIG. 2. (Color online) Field-dependent magnetization measured for magnetic fields applied along the principal axes of  $\text{UCo}_2\text{Si}_2$  at 1.5 K. The inset shows the hysteresis of the field-induced transition.

the jump of the magnetization (the first derivative of the thermodynamic potential), and hysteresis are the basic features of the first-order phase transition. However, the situation is not totally clear and two very close to each other second-order phase transitions cannot be eliminated. As a rule, the order of field-induced transitions in magnets can be checked by considering the temperature-governed transition at the fixed value of the external magnetic field (to see whether such a transition manifests the temperature hysteresis or not). For that purpose one needs to study the temperature dependence of the magnetization,  $M(T)$ , at heating and cooling at the fixed value of the steady magnetic field of the value of 45 T, which is, unfortunately, impossible nowadays. This is why we may assume the first order of the observed transition; however, the possibility of two second-order transitions also cannot be ruled out.

At the transition, the magnetization jumps by  $\Delta M = 0.52 \mu_B$ . This roughly corresponds to 1/3 of the U magnetic moment of  $1.42 \mu_B$  as determined by neutron powder diffraction.<sup>4</sup> Therefore, we may conclude that above  $H_{\text{cr}}$  the anticipated ferrimagnetic state with  $++-$  arrangement is reached. The final transition from this ferrimagnetic to the saturated paramagnetic state (parallel orientation of all magnetic moments) can be expected only at much higher fields. For  $\text{UPd}_2\text{Si}_2$ , e.g., the first magnetization jump with  $\Delta M = 0.75 \mu_B$  at 15 T is followed by a second jump to the saturated magnetization of about  $2.3 \mu_B$  only above 70 T.<sup>11</sup> Based on these data, one might expect that in  $\text{UNi}_2\text{Si}_2$ , where the  $++-$  state is already formed spontaneously, the transition to the saturated state may occur in fields considerably below 70 T. We checked this for  $\text{UNi}_2\text{Si}_2$  but did not observe any sign of such a transition in fields up to 64 T applied along  $c$ . Consequently, an estimate for the critical field leaving the ferrimagnetic state in  $\text{UCo}_2\text{Si}_2$  cannot be made from a simple comparison to the Ni and Pd analogs.

We should mention that we measured only bulk properties whereas for determination of exact magnetic structure one needs microscopic data, in particular, of neutron diffraction experiments, which are impossible to obtain in magnetic fields exceeding 45 T. Therefore we can speak only about an average value of magnetic moments. When we write “ $++-$ ”, we mean first of all that the resulting average moment is 1/3 of individual moment. Then, we use as an argument for the  $++-$  structure the coexistence of  $++-$  and  $+-+-$  structures at different temperatures in the related compound  $\text{UNi}_2\text{Si}_2$ . However, we recognize that a direct transition from the  $++-$  to  $+-+-$  is really difficult to imagine. The simplest way for the transformation from the AF-I structure to the structure with 1/3 moment is from  $+-+-$  to  $+-+-$ . Here only one negative moment changes to positive.

As seen in Fig. 2, the magnetization curve measured along the  $a$  axis is linear up to the highest fields applied without any anomaly. The mentioned small low-field anisotropy in the magnetic susceptibility starts to grow at about 15 T where the  $c$ -axis magnetization exhibits a small positive curvature. Just below the metamagneticlike transition, the magnetization along the  $c$  axis exceeds that along the  $a$  axis already by a factor of 1.5. We think that the positive deviation of the  $c$ -axis curve can be considered as “a precursor” of the transition and reflects reorientation of individual magnetic moments from

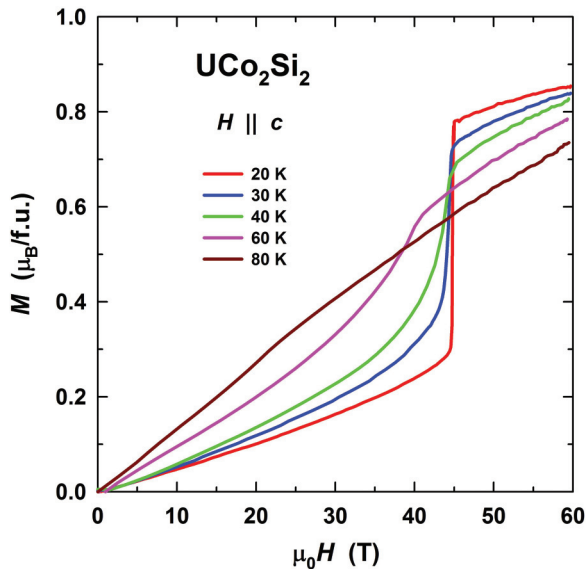


FIG. 3. (Color online) Magnetization as a function of magnetic field applied along the  $c$  axis at elevated temperatures.

“minus” to “plus.” In fact, when the concentration of such defects in AF-I magnetic structure is low, they do not interact. As soon as this concentration reaches some critical value, they start to interact, create nuclei of a new phase, and the transition occurs.

The  $a$ -axis susceptibility of  $3.7 \cdot 10^{-3} \mu_B/T$  per U atom is exactly the same as in  $UNi_2Si_2$  along the  $a$  axis.<sup>8</sup> Such a value is typical for the magnetization along the hard magnetization axis of uranium intermetallic compounds, independent of the crystal structure and type of magnetic ground state. This means that even in ferri- or ferromagnetic U compounds (e.g.,  $UNi_2Si_2$ ) the magnetization process in the hard direction is not a rotation of the spontaneous magnetic moment but reflects mostly the Pauli paramagnetism of the conduction electrons.<sup>1</sup>  $UCo_2Si_2$ , as many other U compounds, behaves as a paramagnet in fields applied perpendicular to the moment direction.

Since the  $a$ -axis magnetization exhibits no anomaly and the magnetic susceptibility along this axis shows only a small temperature dependence,<sup>6</sup> we focus on the  $c$ -axis data in the following. The field-dependent magnetization at elevated temperatures is shown in Fig. 3. The metamagnetic-like transition at 20 K is still very sharp. At higher temperatures, the transition widens and loses the features, characteristic to the first-order one. The transition field,  $H_{cr}$ , determined as the field where the differential susceptibility,  $dM/dH$ , becomes maximal, reduces somewhat with increasing temperature as shown in Fig. 4. The anomalies in  $dM/dH$  become wide and asymmetric. The maxima in  $dM/dH$  have similar magnitude at 1.5 and 20 K ( $1.8$  and  $1.5 \mu_B/T$ , respectively), but drop down to  $0.4 \mu_B/T$  at 30 K and  $0.14 \mu_B/T$  at 40 K (Fig. 5). A very small anomaly in  $dM/dH$  indicating the transition is still observable in the vicinity of 20 T at 80 K. The magnetization gain,  $\Delta M$ , at the transition as well as hysteresis of the transition,  $\Delta H_{cr}$ , decrease monotonically with increasing temperature (Fig. 5).

Figures. 6–8 show that the acoustic properties exhibit pronounced anomalies not only at the magnetic ordering

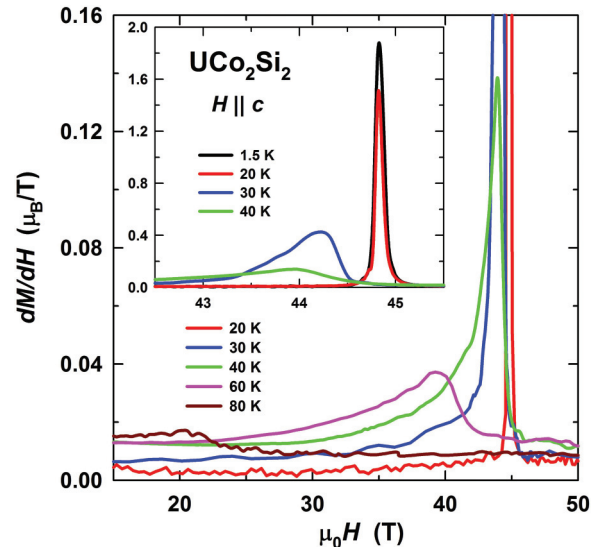


FIG. 4. (Color online) Field dependence of the differential susceptibility,  $dM/dH$ , for magnetic fields applied along the  $c$  axis at different temperatures.

(Fig. 1) but at the metamagnetic-like transition as well. (For clarity of presentation, in Figs. 6–8 we present only field-down branches of the field dependence. The hysteresis is shown separately in Fig. 9.) At 1.5 K, a broad minimum at about 30 T is seen in  $\Delta v/v$  in addition to a sharp 0.6% steplike increase at 45 T where the metamagnetic-like transition occurs (Fig. 6). The origin of the lattice softening at about 30 T is unclear; no features are seen in the magnetization at 30 T. This feature in  $\Delta v/v$  becomes less pronounced at 10 K and disappears at 15 K (Fig. 6). Instead, a strong decrease of  $\Delta v/v$  leading to a deep minimum just before the positive step develops at higher temperatures. At 20 K, the minimum before the step is so large that the total change in  $\Delta v/v$  becomes negative

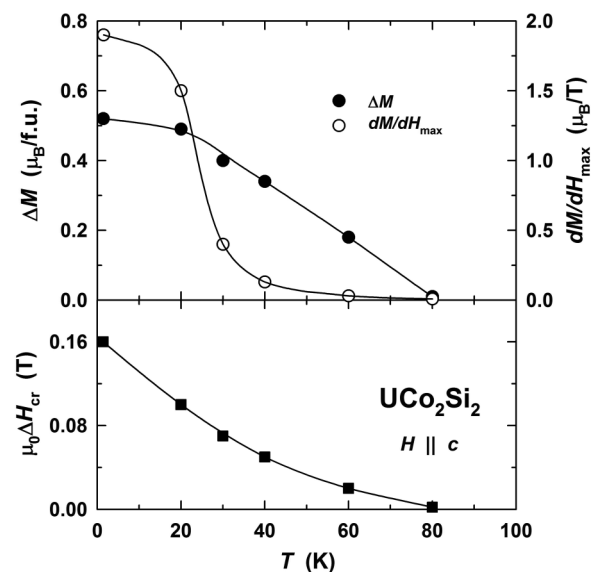


FIG. 5. Temperature dependence of the magnetization gain,  $\Delta M$ , across the metamagnetic transition, maximum of the differential susceptibility at the transition,  $dM/dH_{max}$ , and width of the hysteresis at the transition,  $\Delta H_{cr}$ .

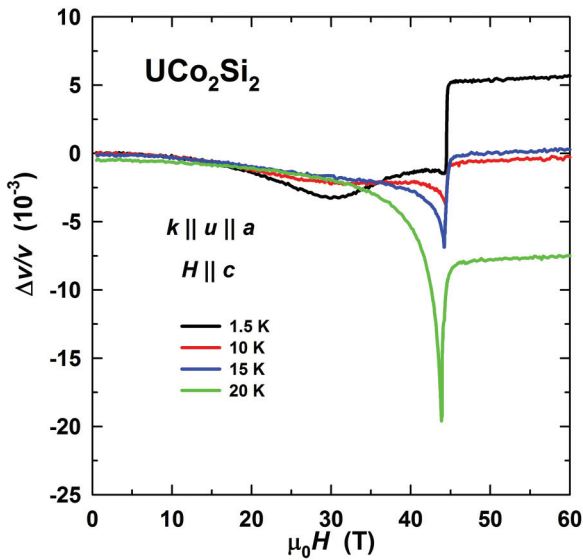


FIG. 6. (Color online) Field dependence of the sound-velocity change,  $\Delta v/v$ , at low temperatures.

up to the maximum field of 60 T, i.e., the 1.5% step does not compensate for the minimum. The minimum is especially deep (4.5%) when the transition changes from the first-order-like behavior to the second-order one at 30 K (Fig. 7). (Note that the scaling of the  $\Delta v/v$  axis in Fig. 7 is different from that in Fig. 6.) Above this temperature, the depth of the minimum reduces and the total change in  $\Delta v/v$  at 60 T becomes positive again at 40 K and above.

The sound attenuation exhibits a very sharp peak at the metamagneticlike transition (Fig. 8). At 1.5 K, the peak is  $\Delta\alpha = 30$  dB/cm which already exceeds the effect observed at the spontaneous transition (Fig. 1) by a factor of 5. The peak grows even further with increasing temperature and reaches the very large value of 110 dB/cm at 20 K. It is still very large at 30 K, 100 dB/cm, and becoming broader. In the isostructural compound  $\text{URu}_2\text{Si}_2$ , a similar peak in  $\Delta\alpha$  at

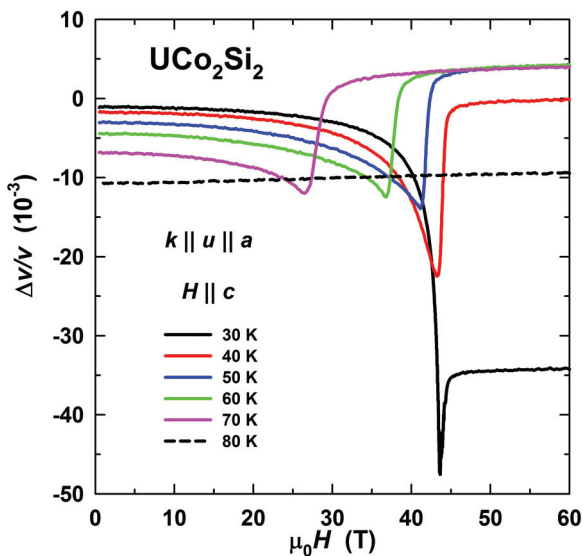


FIG. 7. (Color online) Field dependence of the sound-velocity change,  $\Delta v/v$ , at elevated temperatures.

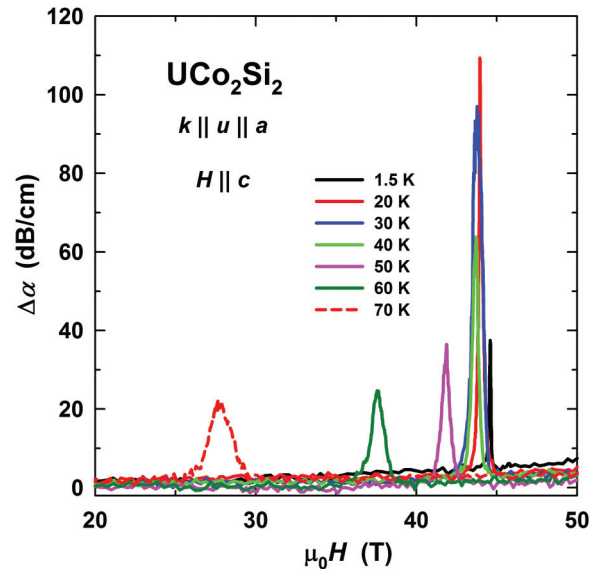


FIG. 8. (Color online) Field dependence of the sound-attenuation change,  $\Delta\alpha$ .

the metamagneticlike transition stays at much lower values of 10 dB/cm (measured in Ref. 18 at 1.5 K in the same geometry as in the present paper).

Figure 9 presents the evolution of the hysteresis of acoustic characteristics at the metamagneticlike transition. The width of the hysteresis is in good agreement with the magnetization results.

The temperature dependences of the acoustic anomalies are presented in Fig. 10. The depth of the minimum and

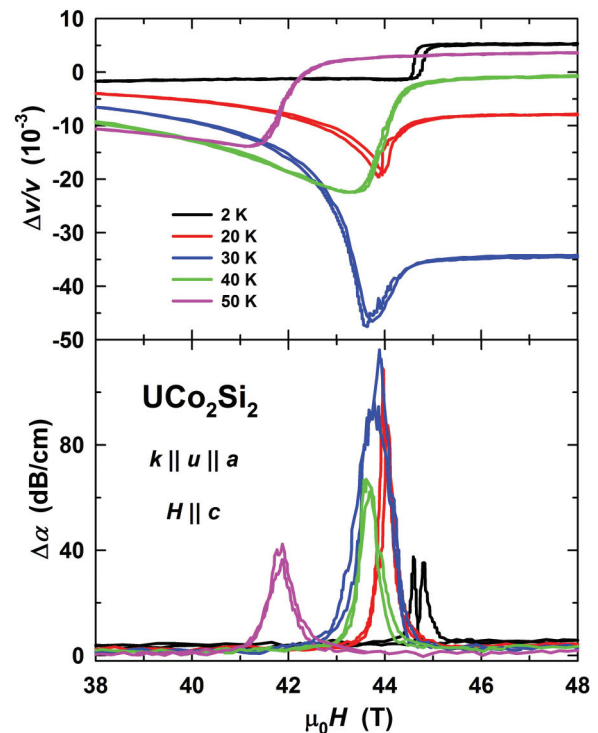


FIG. 9. (Color online) Details of acoustic anomalies at the metamagnetic transition at several temperatures.

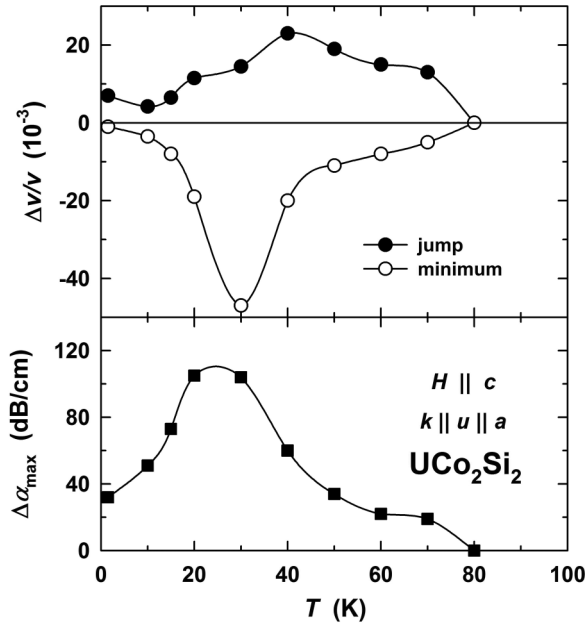


FIG. 10. Temperature dependence of the minimum value of  $\Delta v/v$  before the transition, jump height of  $\Delta v/v$  at the transition, and maximum of  $\Delta\alpha$  at the transition.

the jump height in  $\Delta v/v$  as well as the peak in  $\Delta\alpha$  have a nonmonotonous behavior. The maximum effects appear roughly at the temperature where the metamagneticlike transition changes from first to second order (at about 30 K).

Figure 11 shows the temperature-field phase diagram of  $\text{UCo}_2\text{Si}_2$  in magnetic fields applied along the  $c$  axis. The critical fields of the metamagneticlike transition determined from the magnetoacoustic measurements are in good agreement with data extracted from the magnetization measurements.

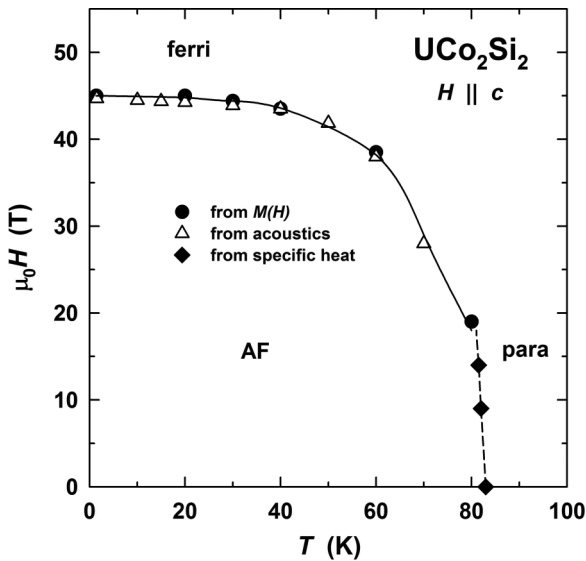


FIG. 11. Magnetic field-temperature phase diagram of  $\text{UCo}_2\text{Si}_2$  in fields applied along the  $c$  axis. The data are obtained from the magnetization (circles), acoustic anomalies in field (triangles), and the temperature dependence of specific heat in different applied field (diamonds, Ref. 6).

$H_{\text{cr}}$  decreases monotonously with increasing temperature and vanishes at  $T_N$ .

Let us now analyze how a renormalization of the exchange constants due to the sound waves in the crystal can affect the sound velocity and attenuation. As shown in Ref. 19 (see also <sup>20,21</sup>) the magnetic-field dependence of the sound-velocity change due to a renormalization of exchange coupling can be presented in the form

$$\begin{aligned} \Delta v &= (\Delta v)_1 + (\Delta v)_2, \\ (\Delta v)_1 &= -[\rho V v (g\mu_B)^4 k^2]^{-1} \left[ 2|g_0(\mathbf{k})|^2 (g\mu_B \langle S_0^z \rangle)^2 \chi_0^z \right. \\ &\quad \left. + T \sum_q \sum_\alpha |g_q(\mathbf{k})|^2 (\chi_q^\alpha)^2 \right], \\ (\Delta v)_2 &= -[2\rho V v (g\mu_B)^2 k^2]^{-1} \left[ h_0^z(\mathbf{k}) (g\mu_B \langle S_0^z \rangle)^2 \right. \\ &\quad \left. + T \sum_q \sum_\alpha h_q^\alpha(\mathbf{k}) \chi_q^\alpha \right], \end{aligned} \quad (1)$$

where the magnetoelastic couplings are defined as

$$g_q^\alpha(\mathbf{k}) = \sum_j e^{iqR_{ji}} (e^{ikR_{ji}} - 1) \mathbf{u}_k \frac{\partial J_{ij}^\alpha}{\partial \mathbf{R}_i}, \quad (2)$$

and

$$h_q^\alpha(\mathbf{k}) = \sum_j e^{-iqR_{ji}} (e^{ikR_{ji}} - 1) (e^{-ikR_{ji}} - 1) \mathbf{u}_k \mathbf{u}_{-k} \frac{\partial^2 J_{ij}^\alpha}{\partial \mathbf{R}_i \partial \mathbf{R}_j}. \quad (3)$$

Here  $\rho$  is the density of the ions,  $V$  is the crystal volume,  $g$  and  $\mu_B$  are the  $g$  factor and Bohr's magneton,  $J_{ij}^\alpha$  is the exchange integral between spins at sites  $i$  and  $j$ ,  $\alpha = x, y, z$ ,  $\mathbf{R}_i$  is the radius vector of the site  $i$ ,  $\mathbf{R}_{ji}$  is the vector connecting the sites  $j$  and  $i$ ,  $\mathbf{k}$  is the wave vector of the sound wave ( $k$  is its absolute value),  $\mathbf{u}_k$  is the vector of sound-wave polarization,  $\langle S_0^z \rangle$  is the average spin moment per site,  $\chi_0^\alpha$  is the homogeneous spin susceptibility, and  $\chi_q^\alpha$  is the inhomogeneous spin susceptibility. We suppose that the main contributions near the phase transition come from the homogeneous susceptibility; hence we can approximately set  $\mathbf{k} = 0$  in  $\chi_k^\alpha$ .

By using this approach, we calculated the magnetic-field dependence of the sound-velocity changes caused by the renormalization of the exchange integrals (Fig. 12). The magnetoelastic couplings of Eqs. (2) and (3) were used as fit parameters. We used data of Fig. 4 for the magnetic-field dependence of the magnetic susceptibility at various temperature values. The main features of the experimentally observed field dependences are well reproduced. In the calculation we correctly observe a softening of the sound velocities at the critical points. However, at fields above  $H_{\text{cr}}$ , the calculated values of the sound-velocity changes are smaller than the experimentally observed data. This deviation may be caused by the neglected contributions of the inhomogeneous terms in the magnetic susceptibility. If this is correct an

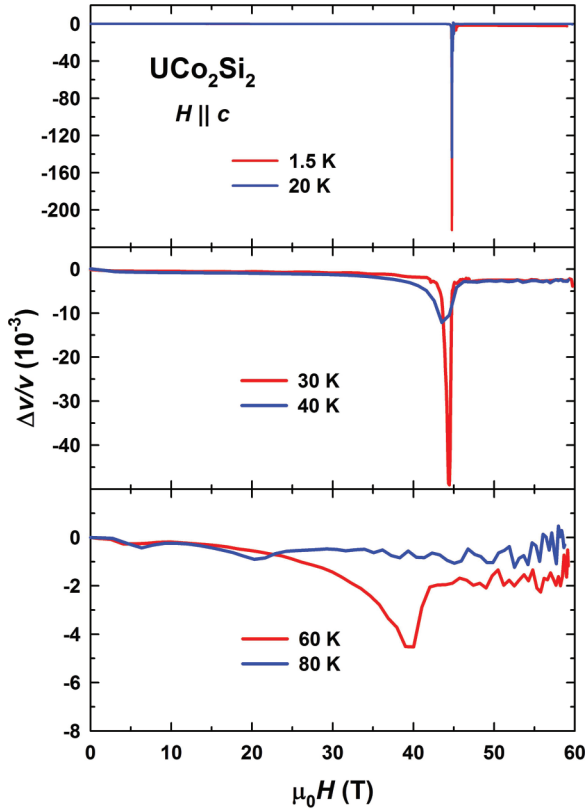


FIG. 12. (Color online) Sound-velocity change in  $\text{UCo}_2\text{Si}_2$  as a function of applied magnetic field for several temperatures, calculated according to Eqs. (1)–(3).

inhomogeneous spin distribution close to the critical field, caused by fluctuations, might be the reason.

The field dependence of the sound attenuation can be calculated by use of the equation<sup>19–21</sup>

$$\Delta\alpha \equiv (\Delta\alpha_k) = [\rho V v (g\mu_B)^4]^{-1} \left[ 2g_0^2(\mathbf{k})(g\mu_B \langle S_0^z \rangle)^2 \chi_0^\alpha A(k) + T \sum_q \sum_\alpha |g_q(\mathbf{k})|^2 (\chi_q^\alpha)^2 B_q(k) \right], \quad (4)$$

where  $A(k) = \gamma_0^z / [(\gamma_0^z)^2 + (vk)^2]$ ,  $B_q(k) = 2\gamma_q^\alpha / [(2\gamma_q^\alpha)^2 + (vk)^2]$ , and the relaxation rates can be approximately written as  $\gamma_0^z = \beta(g\mu_B)^2 / T\chi_0^z$  and  $\gamma_q^\alpha = \beta(g\mu_B)^2 / T\chi_q^\alpha$ , with  $\beta$  being the material-dependent constant.<sup>19</sup> The results of such calculations are presented in Fig. 13. Again, the values of the magnetoelastic coupling and  $\beta$  are used as fit parameters. The calculated data satisfactorily reproduce the main features of the field dependence of the sound attenuation. It turns out that at low temperatures the calculated changes of the sound velocity and attenuation (Figs. 12 and 13) are larger than experimentally observed (Figs. 6–8). This can be explained as follows. From Eqs. (1)–(4) one can see that the changes in the sound velocity and attenuation are connected with the magnetic susceptibility. As presented in Figs. 2–4, the magnetization shows jumps (metamagnetic first-order phase transitions) at low temperatures. Consequently, at these jumps the

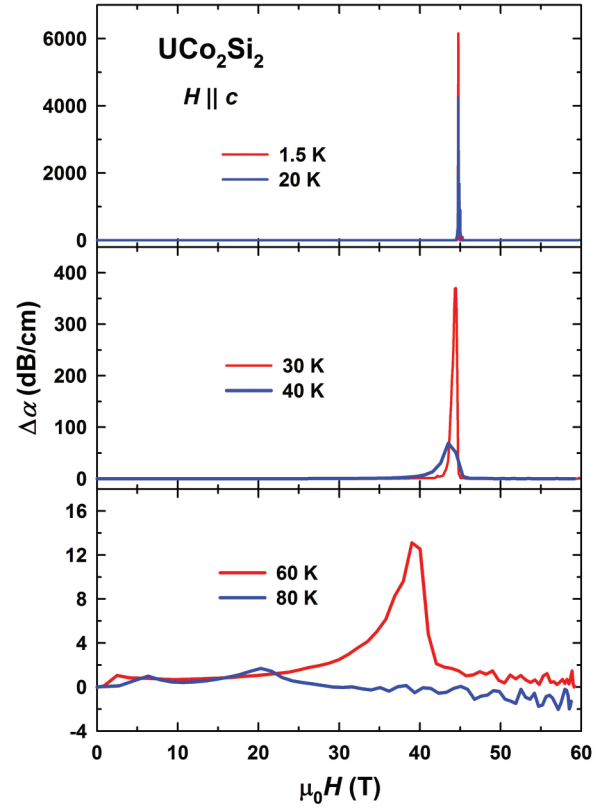


FIG. 13. (Color online) Sound-wave attenuation in  $\text{UCo}_2\text{Si}_2$  as a function of applied magnetic field for several temperatures, calculated according to Eq. (4).

magnetic susceptibility becomes infinite (or, at least, very large). This effect is nicely reproduced by the calculations. Experimentally, effects such as sample inhomogeneities or finite experimental resolution smear out the phase transition and reduce the anomalies both in the susceptibility and the sound-wave properties.

Finally, we can estimate the temperature dependence of the sound-velocity change by  $\Delta v/v = f(E - TC_p)$ ,<sup>22</sup> where the parameter  $f$  is determined by the magnetoelastic couplings, caused by the renormalization of the exchange integral, and  $E$  and  $C_p$  are the internal energy and the specific heat of the magnetic subsystem, respectively. Figure 14 shows

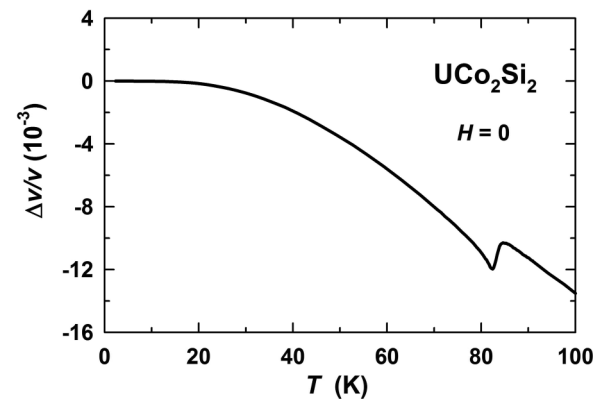


FIG. 14. Calculated temperature dependence of the sound-velocity change in  $\text{UCo}_2\text{Si}_2$  at zero magnetic field.

the calculated temperature dependence of the sound-velocity change. While the overall behavior and the softening of the elastic mode are well reproduced, the absolute value of  $\Delta v/v$  at high temperatures is different from the experiment. Again, we connect this deviation with possible inhomogeneous fluctuations of the magnetic subsystem of  $\text{UCo}_2\text{Si}_2$ .

#### IV. CONCLUSIONS

In the antiferromagnet  $\text{UCo}_2\text{Si}_2$  ( $T_N = 83$  K), the U magnetic moments of  $1.4 \mu_B$  lie along the  $c$  axis of the tetragonal lattice. In magnetic fields applied along this axis, we observed a metamagneticlike transition at 45 T (at 1.5 K). The transition is extremely sharp and exhibits a small but non-negligible hysteresis. With increasing temperature, it becomes broader and vanishes at  $T_N$ . The magnetization gain at the transition corresponds to roughly 1/3 of the U magnetic moment. For this reason, we conclude that the state above the metamagneticlike transition is ferrimagnetic with a  $++-$  arrangement of the magnetic moments, such as in the ground state of the isostructural compound  $\text{UNi}_2\text{Si}_2$ . Our ultrasound measurements confirm this transition, which is accompanied by anomalies in both the sound velocity and sound attenuation. The qualitative agreement between the experimentally observed sound anomalies with calculated data

suggests that the main contribution to the magnetoelastic couplings (at least at low temperatures) comes from the renormalization of the exchange integrals due to sound waves.

Thus, we found that  $\text{UCo}_2\text{Si}_2$  exhibits under certain conditions the  $++-$  phase in addition to the  $+-$  phase. It is difficult to connect appearance of this phase in the compound with expected strength of the  $5f-d$  electron hybridization. It is field induced in  $\text{UCo}_2\text{Si}_2$  with strong hybridization, spontaneous in  $\text{UNi}_2\text{Si}_2$  with lower hybridization, and again field induced in  $\text{UPd}_2\text{Si}_2$  where hybridization is expected to be lowest. But this consideration is based on a very general trend. For deeper understanding, the first-principle band-structure calculations are needed.

#### ACKNOWLEDGMENTS

The single-crystal growth and the static-field magnetization measurements have been performed in the Magnetism and Low-Temperature Laboratories (MLTL, <http://mltl.eu>), which is supported within the program of Czech Research Infrastructures (Project No. LM2011025). Part of the work has been supported by the Czech Science Foundation (Grant No. P204/12/0150) and by EuroMagNET under EU Contract No. 228043. A.A.Z. acknowledges support from the Institute for Chemistry of V. N. Karasin Kharkov National University.

\*Corresponding author: andreev@fzu.cz

<sup>1</sup>V. Sechovský and L. Havela, in *Handbook of Magnetic Materials*, edited by K. H. J. Buschow (Elsevier Science B.V., Amsterdam, 1998), Vol. 11, p. 1, and references therein.

<sup>2</sup>A. Szytula and J. Leciejewicz, in *Handbook on the Physics and Chemistry of the Rare Earths*, edited by K. A. Gschneider, Jr. and L. Eyring (Elsevier Science B.V., Amsterdam, 1989), Vol. 12, p. 133, and references therein.

<sup>3</sup>J. A. Mydosh and P. M. Oppeneer, *Rev. Mod. Phys.* **83**, 1301 (2011).

<sup>4</sup>L. Chelmicki, J. Leciejewicz, and A. Zygmunt, *J. Phys. Chem. Solids* **46**, 529 (1985).

<sup>5</sup>M. Mihalik, O. Kolomiets, J.-C. Griveau, A. V. Andreev, and V. Sechovský, *J. Phys. Soc. Jpn.* **76** (Suppl. A), 54 (2007).

<sup>6</sup>M. Mihalik, A. Kolomiets, J.-C. Griveau, A. V. Andreev, and V. Sechovský, *High Press. Res.* **26**, 479 (2006).

<sup>7</sup>L. Rebelsky, H. Lin, M. W. McElfresh, M. F. Collins, J. D. Garrett, W. J. L. Buyers, and M. S. Torikachvili, *Phys. B* **180-181**, 43 (1992).

<sup>8</sup>F. Honda, G. Oomi, T. Kagayama, A. V. Andreev, V. Sechovský, L. Havela, M. I. Bartashevich, T. Goto, and A. A. Menovsky, *J. Magn. Magn. Mater.* **177-181**, 49 (1998).

<sup>9</sup>F. Honda, A. V. Andreev, V. Sechovský, Y. Homma, and Y. Shiokawa, *Eur. Phys. J. B* **30**, 313 (2002).

<sup>10</sup>T. Honma, H. Amitsuka, T. Sakakibara, K. Sugiyama, and M. Date, *Phys. B* **186-188**, 684 (1993).

<sup>11</sup>T. Honma, H. Amitsuka, S. Yasunami, K. Tenya, T. Sakakibara, H. Mitamura, T. Goto, G. Kido, S. Kawarazaki, Y. Miyako, K. Sugiyama, and M. Date, *J. Phys. Soc. Jpn.* **67**, 1017 (1998).

<sup>12</sup>A. V. Andreev, Y. Skourski, S. Yasin, S. Zherlitsyn, and J. Wosnitza, *J. Magn. Magn. Mater.* **324**, 3413 (2012).

<sup>13</sup>K. H. J. Buschow and D. B. de Mooij, *Philips J. Res.* **41**, 55 (1986).

<sup>14</sup>Y. Skourski, M. D. Kuz'min, K. P. Skokov, A. V. Andreev, and J. Wosnitza, *Phys. Rev. B* **83**, 214420 (2011).

<sup>15</sup>B. Wolf, B. Lüthi, S. Schmidt, H. Schwenk, M. Sieling, S. Zherlitsyn, and I. Kouroudis, *Phys. B* **294-295**, 612 (2001).

<sup>16</sup>S. Yasin, A. V. Andreev, Y. Skourski, J. Wosnitza, S. Zherlitsyn, and A. A. Zvyagin, *Phys. Rev. B* **83**, 134401 (2011).

<sup>17</sup>G. Quirion, A. Kelly, S. Newbury, F. S. Razava, and J. D. Garrett, *Can. J. Phys.* **81**, 797 (2003).

<sup>18</sup>T. Yanagisawa, S. Mombetsu, H. Hidaka, H. Amitsuka, M. Akatsu, S. Yasin, S. Zherlitsyn, J. Wosnitza, K. Huang, and M. B. Maple, *J. Phys. Soc. Jpn.* **82**, 013601 (2013).

<sup>19</sup>M. Tachiki and S. Maekawa, *Prog. Theor. Phys.* **51**, 1 (1974).

<sup>20</sup>O. Chiatti, A. Sytcheva, J. Wosnitza, S. Zherlitsyn, A. A. Zvyagin, V. S. Zapf, M. Jaime, and A. Paduan-Filho, *Phys. Rev. B* **78**, 094406 (2008).

<sup>21</sup>A. Sytcheva, O. Chiatti, J. Wosnitza, S. Zherlitsyn, A. A. Zvyagin, R. Coldea, and Z. Tylczynski, *Phys. Rev. B* **80**, 224414 (2009).

<sup>22</sup>S. Bhattacharjee, S. Zherlitsyn, O. Chiatti, A. Sytcheva, J. Wosnitza, R. Moessner, M. E. Zhitomirsky, P. Lemmens, V. Tsurkan, and A. Loidl, *Phys. Rev. B* **83**, 184421 (2011).